Relative Biological Effectiveness of HZE Fe Ions for Induction of Micro-Nuclei at Low Doses.

Torsten Groesser, Eugene Chun and Bjorn Rydberg[1]

Lawrence Berkeley National Laboratory, Life Sciences Division, Building 74-157, 1 Cyclotron Road, Berkeley, CA 94720.

Running title: RBE of Fe ions for induction of micronuclei

[1] Address for correspondence: Lawrence Berkeley National Laboratory, Life Sciences Division, Building 74-157, 1 Cyclotron Road, Berkeley, CA 94720; email: berydberg@lbl.gov

Abstract

Groesser, T., Chun, E. and Rydberg, B. Relative Biological Effectiveness of HZE Fe Ions for Induction of Micro-Nuclei at Low Doses. *Radiat. Res.*

Dose-response curves for induction of micro-nuclei (MN) was measured in Chinese hamster V79 and xrs6 (Ku80-) cells and in human mammary epithelial MCF10A cells in the dose range of 0.05 – 1 Gy. The Chinese Hamster cells were exposed to 1 GeV/u Fe ions, 600 MeV/u Fe ions, and 300 MeV/u Fe ions (LETs of 151, 176 and 235 keV/µm respectively) as well as with 320 kVp X-rays as reference. Second-order polynomials were fitted to the induction curves and the initial slopes (the alpha values) were used to calculate RBE. For the repair proficient V79 cells the RBE at these low doses increased with LET. The values obtained were 3.1 (LET=151 keV/µm), 4.3 (LET = 176 keV/µm) and 5.7 (LET = 235 keV/µm), while the RBE was close to 1 for the repair deficient xrs6 cells regardless of LET. For the MCF10A cells the RBE was determined for 1 GeV/u Fe ions and found to be 5.4, slightly higher than for V79 cells. To test the effect of shielding, the 1 GeV/u Fe ion beam was intercepted by various thickness of high-density polyethylene plastic absorbers, which resulted in energy loss and fragmentation. It was found that the MN yield for V79 cells placed behind the absorbers decreased in proportion to the decrease in dose both before and after the Fe ion Bragg peak (excluding the area around the Fe-ion Bragg peak itself), indicating that RBE did not change significantly due to shielding. At the Bragg peak the effectiveness for MN formation per unit dose was decreased, indicating an “overkill” effect by low-energy very high-LET Fe ions.

INTRODUCTION

Estimation of risk from Highly charged (Z) high Energy (HZE) ions in the space environment depends critically on measured values of the Relative Biological Effectiveness (RBE) for cancer induction and other endpoints (*1, 2*). Of particular concern is the deep penetration of such high LET particles to all organs of the body, a situation not experienced in the earth environment. Published values of RBE as a function of Linear Energy Transfer (LET) are highly variable, particularly for low doses, see (*2*) for summary. Ionizing radiation is predominantly a clastogenic agent, and cytogenetic endpoints are therefore highly relevant as they are implicated as being involved in carcinogenesis. Since RBE for most endpoints has been found to depend on dose, of particular interest for risk estimation is the RBE at the lowest doses possible, generally the maximum RBE (RBE_{max} or the Q-value).

Micronuclei (MN) formation has been used previously to assess cytogenetic damage induced by HZE ions. Brooks *et* al. (*3, 4*) studied MN induction *in vivo* in the trachea and deep lung of the rat, and obtained RBE values of 0.9 to 3.3 for 1 GeV/u Fe ions, with ^{60}Co gamma rays as reference radiation. A similar RBE of 3.2 was measured for chromosome aberrations in bone marrow cells. These are much lower RBE values than previously observed for alpha particles with similar LET from radon daughters. This suggests that track structure parameters other than LET are of importance. The authors suggest that cells traversed by Fe ions are often killed or blocked in the cell cycle and not contributing to the cells that divide and give rise to MN, thus giving a bias to cells that were traversed only by secondary low LET δ-rays. To what extent this is the case will depend on the cell system under study, in particular it will depend on the radiation sensitivity for cell killing. For the study of chromosome aberrations from HZE ions (*5, 6*), most studies have been done with human lymphocytes, a radiation sensitive cell type with regard to apoptosis. Probably, results with lymphocytes may not be representative for more radioresistant cell types, particularly not for high LET radiations where a single hit will produce a significant, potentially cell killing dose to the cell. In this paper we

study RBE for Fe ion radiation in more radioresistant cell types in the dose range of 0.05 to 1 Gy.

MATERIALS AND METHODS

Cells and cell culture

Chinese hamster lung fibroblast V79 and DNA double-strand break repair-deficient Chinese hamster ovary cell line xrs6 (deficient in Ku80) were cultured in α-MEM medium (Gibco) with 10% FBS (Gibco), 2 mM L-glutamine (Gibco), 100 Units/ml penicillin: streptomycin solution plus 0.25 μg/ml Amphotericin B as Fungizone (Gibco), and 10 mM Hepes buffer (Sigma). The human mammary epithelial cells MCF10A (*7*) were cultured in serum free MEBM medium (with bicarbonate and phenol red; Cambrex) with 70 μg/ml BPE, 5ng/ml hEGF, 0.5 μg/ml Hydrocortisone, 5 μg/ml Insulin (SingleQuot®Kit; Cambrex), and 100 ng/ml Cholera toxin (Sigma).
Cells were cultured in 25 cm^2 or 75 cm^2 tissue culture flasks (Gibco) and incubated at 37°C under 5% CO_2 and 95% humidity. For passage, V79 and xrs6 cells were trypsinized at 37°C for 3-5 min and trypsinization was stopped by adding medium. MCF10A cells were washed twice with trypsin and trypsinization was stopped using soybean trypsin inhibitor (1mg/ml; Sigma). After the cells detached from the flask they were washed once in PBS before reseeded in appropriate numbers.

Irradiations

Cells in exponential growth were exposed to Fe ions at the NSRL radiation facility at Brookhaven National Laboratory. Precise dosimetry was carried out as described (*8*). For the experiments with shielding, high density polyethylene plastic of various thickness was inserted in the beam. A CCD camera that viewed a fluorescent screen behind the cell culture flasks (a regular part of the beam-line setup) was used to

image the cell culture flasks during radiation. Using this system it was possible to fine-tune the absorber thickness to position the Bragg peak exactly at the cell layer.

X-irradiation was performed with 320 kVp X-rays with 0.5 mm copper filtration. A calibrated ion chamber with temperature and pressure correction (RadCal corporation) was used for dosimetry. Each experiment was carried out with a minimum of triplicate samples.

Micronucleus assay

The cytokinesis-block micronucleus assay (*9*) was used. Cytochalasin-B at a concentration of 6 μg/ml was added directly after exposure, followed by 24 hr incubation at 37°C (Chinese Hamster cells) or 48 hr incubation at 37°C (human MCF10A cells).
The cells were then trypsinized, centrifuged, and resuspended in 7 ml 0.075 M potassium chloride for 10 min at 37°C. Fixation was performed by adding 3 ml of 100% methanol to each centrifuge tube and incubating the cells for at least 1h at room temperature, followed by fixation twice in acetic acid/methanol (1:3). Fixed cells were either cyto-spun onto glass slides or dropped onto wet slides. The Chinese Hamster cells were stained with Diff Quick (Dade Behring) following the manufacture's protocol. Because of a more prominent cytoplasm, the human MCF10A cells were better stained with 10μg/ml Acridine Orange (AO) in PBS. The slides were coded and scored blindly. For each sample, micronuclei induction in 1000 binucleated cells was scored following the scoring criteria described in detail in Fenech *et al*. (*9*). Examples of micro-nuclei are given in Fig. 1.

RESULTS

Doses and Fluences

The experiments were performed using Fe ion irradiation at doses of 0.05 Gy –1.0 Gy. To determine the number of hits per cell nucleus at these doses, nuclear areas of live cells were measured by labeling with Hoechst 33342 and using image analysis software. Table 1 shows the results including average number of hits per cell for the different doses and Fe ion energies. As seen, for doses below 0.1 Gy cells typically experienced a single traversal. This is the most relevant situation for risk estimation in space environments.

Induction of micronuclei in DSB repair competent cells

Micronuclei formation was measured in Chinese hamster V79 cells exposed to three different energies of Fe ions and to X-rays, with emphasis given to low doses below 0.5 Gy. Results are shown in Figure 2, left panels. At least triplicate determinations were carried out, and the data were fitted with second order polynomials. The initial slope at low doses were determined by the linear coefficient (alpha value) and RBE was calculated by comparing the alpha values for X-rays and for the respective Fe ions. As shown in Table 2 and Figure 3, the RBE increased with increasing LET from 3.1 to 5.7.

For 1 GeV/u Fe ions, micronuclei induction was also measured in the human MCF10A mammary epithelial cell line (Figure 4). A value of RBE = 5.4 was obtained, slightly above the value for V79 cells for the same Fe ion energy. The higher value reflected mainly a lower MN induction value for X-rays rather than a higher value for Fe ions, as seen in Table 2.

Induction of micronuclei in DSB repair deficient cells

MN induction was also measured in the DSB repair deficient Chinese hamster xrs6 cell line (Figure 1, right panels). These cells had a high MN induction rate for X-rays, reflecting its inability to repair DSBs. However the induction rate for Fe-ions was generally slightly lower than for X-rays, with the initial induction rate (alpha value) similar to X-rays, resulting in RBE values close to unity (Table 1 and Figure 3).

Effect of shielding

To test the effect of shielding, various amounts (0–30 cm) of high-density (tissue-equivalent) polyethylene absorbers were inserted between the 1 GeV/u Fe ion beam and the targets in the form of V79 or xrs6 sample cell culture flasks. The same absorbers were also used to obtain the dose as a function of absorber thickness (Bragg curve). For each exposure the dose was set at 0.5 Gy at the entrance of the absorbers, and the dose to the samples were determined by the Bragg curve. As seen in Figure 5, the MN induction frequency as a function of absorber thickness was proportional to dose with the exception of the Fe ion Bragg peak.

DISCUSSION

Micronuclei formation is believed to reflect the presence of acentric fragments or to a lesser extent reflect other types of mitotic failure. In both cases, genomic material left behind in anaphase may not be included in one of the daughter nuclei but form separate micronuclei. Acentric fragments often occur in conjunction with formation of dicentric chromosomes, and dicentrics are believed to occur with the same yield as translocations. From this point of view, MN formation can be seen as a diagnistic tool for cytogenetic damage in general, both those that often are regarded mainly as being lethal (dicentrics) as well as those that are regarded mainly as easily propagated to the progeny (translocations). Since acentric fragments way also be incorporated in one or the other

daughter nuclei, both deletions and duplications may result, both typical of radiation-induced cancer cells as recently indicated by CGH analysis (*10*). We therefore consider MN formation to be a relevant endpoint to measure the clastogenic potential of different radiations with relevance to carcinogenesis.

From a practical point of view, MN formation is a more sensitive assay than the evaluation of chromosome aberrations in metaphase spreads. This is due to the ease and quickness of scoring, allowing for a better statistical accuracy. In the present work, the induction curves were each the result of scoring 24,000 binucleated cells (blindly) at a speed of about 2000 cells per hour by an experienced scorer. This allowed us to get a good estimation of RBE at doses below 0.3 Gy, when typically cells are traversed by single tracks from the high LET radiations tested. This situation is much more relevant to the situation in space travel than the use of higher doses when cells typically are traversed by multiple tracks.

The main body of work previously assessing the RBE for cytogenetic damage from HZE particle radiation has been carried out mainly using human lymphocytes as the cell system of study (*5, 6*). It can be pointed out that such cells are radiosensitive, particularly with respect to apoptosis. As a result, the "overkill" effect that is believed to be responsible for the lowering of observable biological effect at very high LETs, will come into effect at lower LETs than for more radioresistant cells. This probably explains why the maximum cytogenetic damage in the lymphocytes was observed for 1 GeV/u Fe ions (LET=150 keV/μm), with declining RBE for increasing LETs, while for the V79 cells in this study we observed a continuous increase of RBE at least up to LET=250 keV/μm (for 300 MeV/u Fe ions). It is clear that RBE/LET relationships will depend on cell type for this reason, and a single universal relationship of a "quality-factor" as a function of LET is an oversimplification.

Durante *et al.* (*5*) studied extensively the effect of shielding on the induction of chromosome aberrations in human lymphocytes. They point out that despite the fact that the primary 1 GeV/u Fe ions fragment extensively into lighter ions as they pass through

the shielding material, the dose-average LET does not change dramatically with shielding thickness. Surprisingly, they observed nevertheless a dramatic reduction of aberration frequency per unit dose as a function of shielding thickness for 1 GeV Fe ions that was not observed with 500 MeV/u Fe ions. They suggest that factors related to track structure other than LET must be taken into account. However, in the present work with V79 cells we could not reproduce this result. In our hands with our cell system, we find the effectiveness per unit dose for MN induction to be nearly independent of shielding thickness, as would be expected if dose-average LET does not change to a large extent. The reduction in MN induction we observe could be explained exclusively by the reduction in dose with the exception of the Bragg peak, where the effectiveness was lower. It is estimated that that 89% of the primary Fe ions fragment into lighter ions during passage through the absorbers and that the remaining 11% will stop at the Bragg peak with LET values of several thousand keV/μm. A similar reduction of the effectiveness at the Bragg peak was recently reported by Wu et al. (*11*) for MN induction in primary human lymphocytes.

For the DSB repair deficient xrs6 cells, we obtain RBE values close to 1. This was mainly caused by an increase of MN formation for X-rays compared to repair proficient cells, without a similar increase for the high LET Fe ions. This result is very similar to what has been observed previously for cell survival (*12*). Apparently, when the cells cannot repair DSBs, the breaks are equally effective for high and low LET. On the other hand, repair proficient cells can handle the breaks from low LET radiation much better than breaks from high LET radiation, presumably due to differences in DSB complexity.

Among previously measured RBE values of relevance for the space environment (*2*), the values for MN induction obtained here (for repair proficient cells) fall on the lower end of the spectrum. For induction of cancer in rodents, in particular for tumors in the harderian gland as studied by Alpen *et al.* (*13, 14*), much higher RBE values up to RBE = 40 have been recorded. However, the generality of such high RBE values for human cancers is not known.

ACKNOWLEDGEMENTS

We thank Dr. Marcelo Vazquez, Dr. Betsy Sutherland, and Dr. Adam Rusek and their groups for support during the NSRL runs at Brookhaven National Laboratory, and Dr. Lawrence Heilbronn for fragmentation analysis. The research was funded by NASA Grant no. T9493W (awarded to Dr. Bjorn Rydberg) and NASA Grant no. T6275W (awarded to Dr. Mary-Helen Barcellos-Hoff, NSCOR).

REFERENCES

1. F. A. Cucinotta and M. Durante, Cancer risk from exposure to galactic cosmic rays: implications for space exploration by human beings. *Lancet Oncol* **7**, 431-435 (2006).

2. F. A. Cucinotta, W. Schimmerling, J. W. Wilson, L. E. Peterson, G. D. Badhwar, P. B. Saganti and J. F. Dicello, Space radiation cancer risks and uncertainties for Mars missions. *Radiat Res* **156**, 682-688 (2001).

3. A. Brooks, S. Bao, K. Rithidech, L. A. Couch and L. A. Braby, Relative effectiveness of HZE iron-56 particles for the induction of cytogenetic damage in vivo. *Radiat Res* **155**, 353-359 (2001).

4. A. L. Brooks, S. Bao, K. Rithidech, W. B. Chrisler, L. A. Couch and L. A. Braby, Induction and repair of HZE induced cytogenetic damage. *Phys Med* **17 Suppl 1**, 183-184 (2001).

5. M. Durante, K. George, G. Gialanella, G. Grossi, C. La Tessa, L. Manti, J. Miller, M. Pugliese, P. Scampoli and F. A. Cucinotta, Cytogenetic effects of high-energy iron ions: dependence on shielding thickness and material. *Radiat Res* **164**, 571-576 (2005).

6. K. George, M. Durante, V. Willingham, H. Wu, T. C. Yang and F. A. Cucinotta, Biological effectiveness of accelerated particles for the induction of chromosome damage

measured in metaphase and interphase human lymphocytes. *Radiat Res* **160**, 425-435 (2003).

7. H. D. Soule, T. M. Maloney, S. R. Wolman, W. D. Peterson, Jr., R. Brenz, C. M. McGrath, J. Russo, R. J. Pauley, R. F. Jones and S. C. Brooks, Isolation and characterization of a spontaneously immortalized human breast epithelial cell line, MCF-10. *Cancer Res* **50**, 6075-6086 (1990).

8. C. Zeitlin, L. Heilbronn and J. Miller, Detailed characterization of the 1087 MeV/nucleon iron-56 beam used for radiobiology at the alternating gradient synchrotron. *Radiat Res* **149**, 560-569 (1998).

9. M. Fenech, W. P. Chang, M. Kirsch-Volders, N. Holland, S. Bonassi and E. Zeiger, HUMN project: detailed description of the scoring criteria for the cytokinesis-block micronucleus assay using isolated human lymphocyte cultures. *Mutat Res* **534**, 65-75 (2003).

10. J. H. Mao, J. Li, T. Jiang, Q. Li, D. Wu, J. Perez-Losada, R. DelRosario, L. Peterson, A. Balmain and W. W. Cai, Genomic instability in radiation-induced mouse lymphoma from p53 heterozygous mice. *Oncogene* **24**, 7924-7934 (2005).

11. H. Wu, M. Hada, J. Meador, X. Hu, A. Rusek and F. A. Cucinotta, Induction of micronuclei in human fibroblasts across the Bragg curve of energetic heavy ions. *Radiat Res* **166**, 583-589 (2006).

12. R. Okayasu, M. Okada, A. Okabe, M. Noguchi, K. Takakura and S. Takahashi, Repair of DNA damage induced by accelerated heavy ions in mammalian cells proficient and deficient in the non-homologous end-joining pathway. *Radiat Res* **165**, 59-67 (2006).

13. E. L. Alpen, P. Powers-Risius, S. B. Curtis and R. DeGuzman, Tumorigenic potential of high-Z, high-LET charged-particle radiations. *Radiat Res* **136**, 382-391 (1993).

14. E. L. Alpen, P. Powers-Risius, S. B. Curtis, R. DeGuzman and R. J. Fry, Fluence-based relative biological effectiveness for charged particle carcinogenesis in mouse Harderian gland. *Adv Space Res* **14**, 573-581 (1994).

Tables.

Traversals per Nucleus										
Cell type	**Nuclear area**	**Fe ion energy** (GeV/u)	**LET** (keV/μm)	**Dose** (Gy)						
				0.05	**0.075**	**0.1**	**0.2**	**0.3**	**0.5**	**1**
V79	150 μm^2	1.0	151	*0.31*	*0.46*	*0.62*	*1.2*	*1.9*	*3.1*	*6.2*
		0.6	176	*0.27*	*0.39*	*0.53*	*1.0*	*1.6*	*2.7*	*5.3*
		0.3	235	*0.20*	*0.30*	*0.40*	*0.77*	*1.2*	*2.0*	*4.0*
xrs6	110 μm^2	1.0	151	*0.23*	*0.34*	*0.45*	*0.90*	*1.4*	*2.3*	*4.6*
		0.6	176	*0.20*	*0.29*	*0.39*	*0.77*	*1.2*	*2.0*	*3.9*
		0.3	235	*0.15*	*0.22*	*0.29*	*0.58*	*0.9*	*1.5*	*3.0*
MCF10A	179 μm^2	1		*0.37*	*0.56*	*0.74*	*1.5*	*2.2*	*3.7*	*7.4*

Table 1. Average number of traversals/nucleus for the various cells and doses used (calculated as = 6.24 * Dose(Gy) *area (μm^2) / LET(keV/μm)). The nuclear areas were measured using Hoechst 33342 staining on live cells.

	LET	V79 cells		xrs6 cells		MCF-10A cells	
Irradiation	(keV/μm)	linear coeff	RBE	linear coeff	RBE	linear coeff	RBE
X-rays	N/A	7.26	1	43.3	1	4.19	1
1 GeV/n Fe	151	22.6	3.11	42.7	0.98	22.7	5.42
600 MeV/n Fe	176	31.5	4.34	33.4	0.77	-	-
300 MeV/n Fe	235	41.4	5.71	39.4	0.91	-	-

Table 2. The initial slope (alpha value) for number of MN per 100 cells per Gy (linear coefficient of fitted polynomial) and RBE_{max} for the different cell lines and LETs.

Figure legends.

Fig 1. Microphotographs of binucleated (Cytochalasin-B treated) Chinese Hamster V79 cells stained with Diff Quick (top left without micronucleus, top right with micronucleus) and human MCF10A cells stained with Acridine Orange (bottom left and right, both with one micronucleus).

Fig. 2. Micronuclei formation as a function of dose for V79 cells (left panels) and xrs6 cells (right panels). The Fe ion energy (1GeV/u, 600 MeV/u or 300 MeV/u) are as indicated in each panel. Results for X-rays are shown by the dotted line in each graph. Error bars are standard error of the mean from at least 3 independent cell culture flasks. The lines are second order polynomials fitted to the data. The initial slopes of these polynomials (α-values) are used to calculate RBE.

Fig. 3. RBE as a function of LET for micronuclei formation in V79 cells (normal DSB repair) and xrs6 cells (deficient in NHEJ). Results are for Fe ion irradiation compared to 300 kVp X-rays.

Fig. 4. Micronucleus formation in human MCF10A cells as a function of dose for 1 GeV/u Fe ions (solid line) and for X-rays (dotted line). Error bars are standard error of the mean from 3 independent cell culture flasks. The lines are second order polynomials fitted to the data. The initial slopes of these polynomials (α-values) are used to calculate RBE.

Fig. 5. Micronucleus formation as a function of shielding thickness. Various amounts of high-density polyethylene plastic were inserted between the Fe ion beam (1 GeV/u) and

the cell culture flask. The dose at the entrance of the shielding was 0.5 Gy and the dose at the sample was dependent of the shielding thickness as indicated by the dotted line (Bragg curve, right axis). The micronuclei induction (left axis) shows the average value for three cell culture flasks with standard error of the mean. The values for non-irradiated controls have been subtracted. The unfragmented Fe ions stopped at the Bragg peak at 24.8 cm, while fragments penetrated further (to the right of the Bragg peak). Top graph: V79 cells, bottom graph: xrs6 cells.

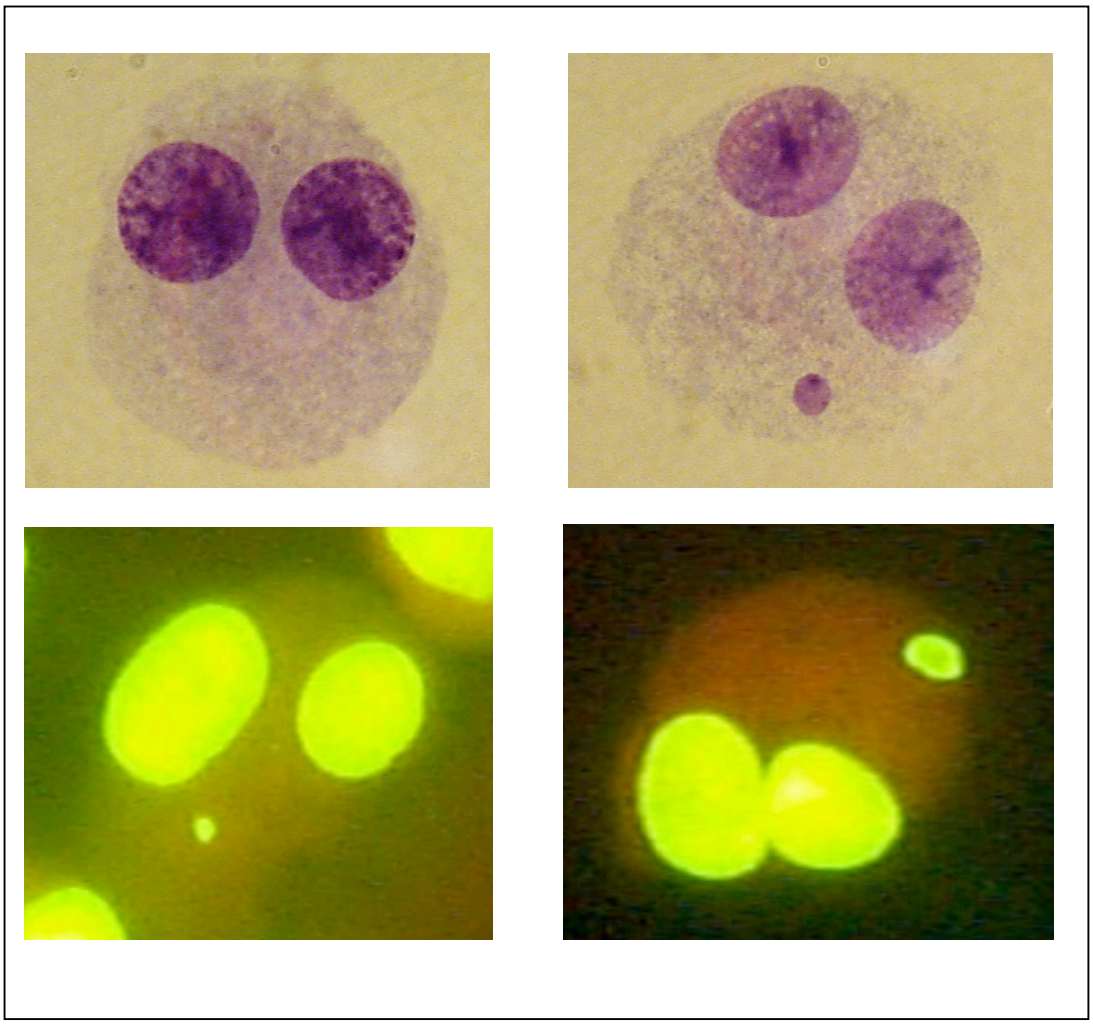

Figure 1

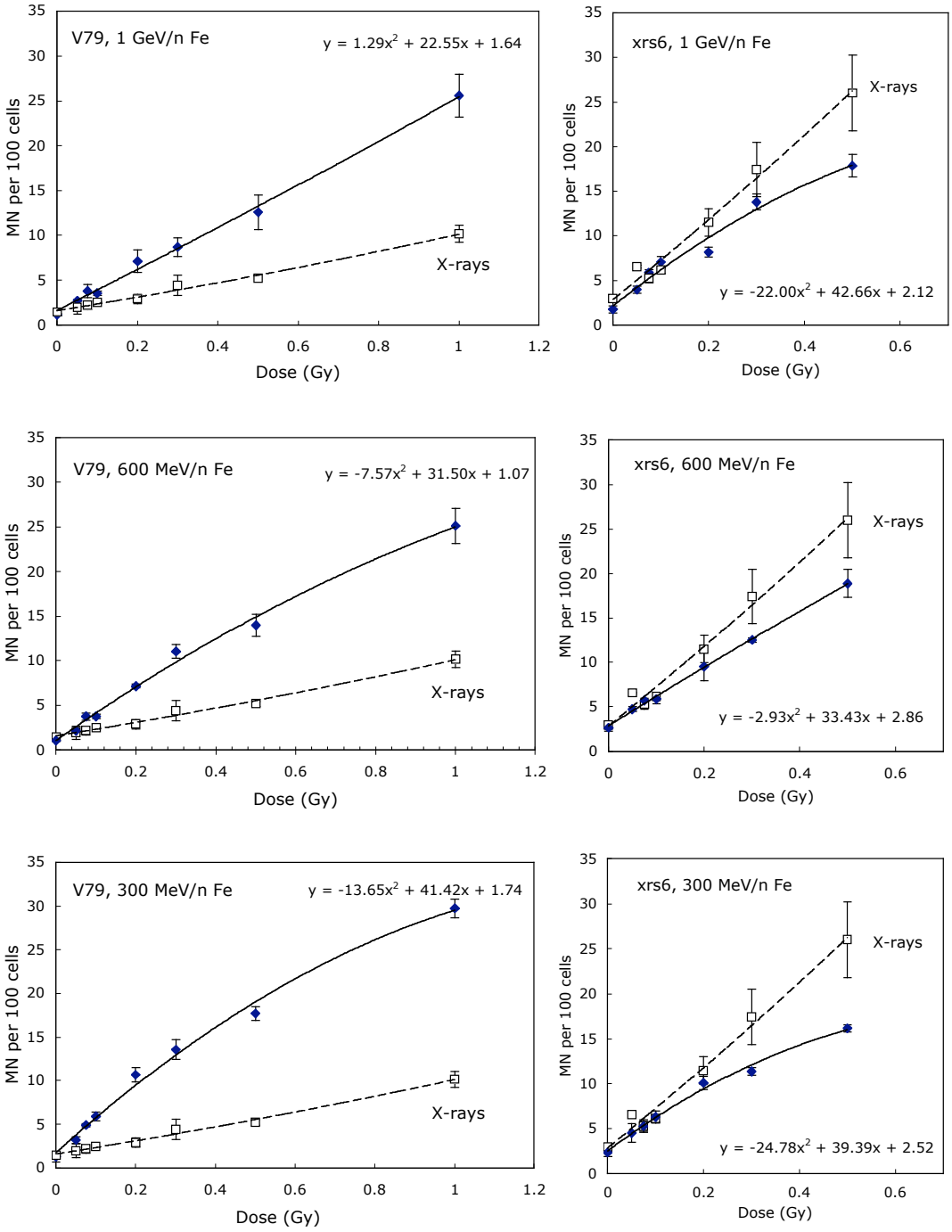
V79, 1 GeV/n Fe
y = 1.29x² + 22.55x + 1.64
X-rays
xrs6, 1 GeV/n Fe
X-rays
y = -22.00x² + 42.66x + 2.12
V79, 600 MeV/n Fe
y = -7.57x² + 31.50x + 1.07
X-rays
xrs6, 600 MeV/n Fe
X-rays
y = -2.93x² + 33.43x + 2.86
V79, 300 MeV/n Fe
y = -13.65x² + 41.42x + 1.74
X-rays
xrs6, 300 MeV/n Fe
X-rays
y = -24.78x² + 39.39x + 2.52
MN per 100 cells
Dose (Gy)

Figure 2.

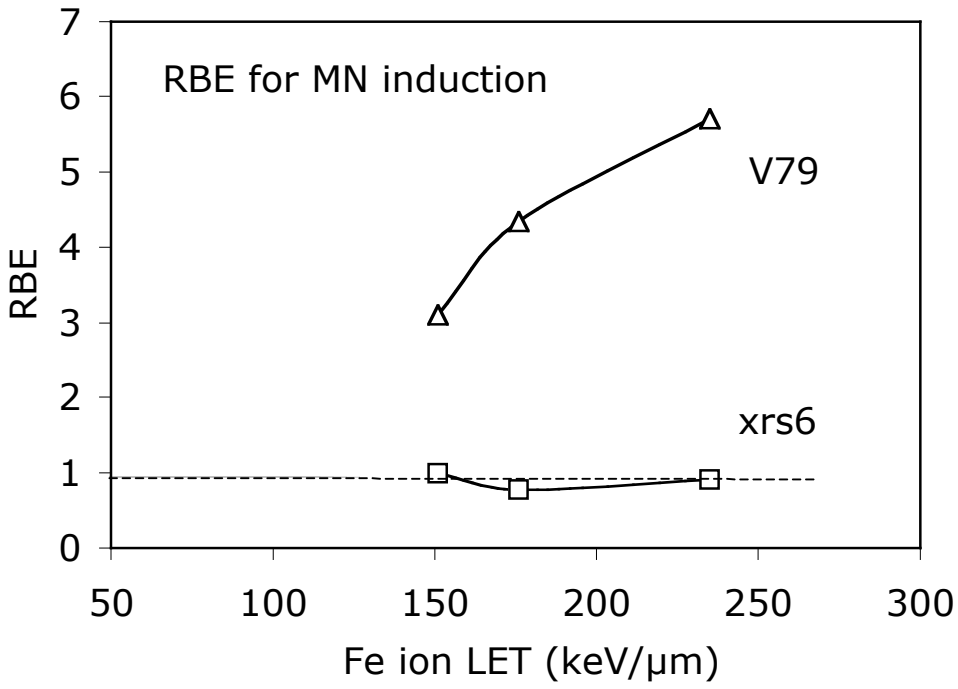
RBE for MN induction
V79
xrs6
RBE
Fe ion LET (keV/μm)
0
1
2
3
4
5
6
7
50
100
150
200
250
300

Figure 3.

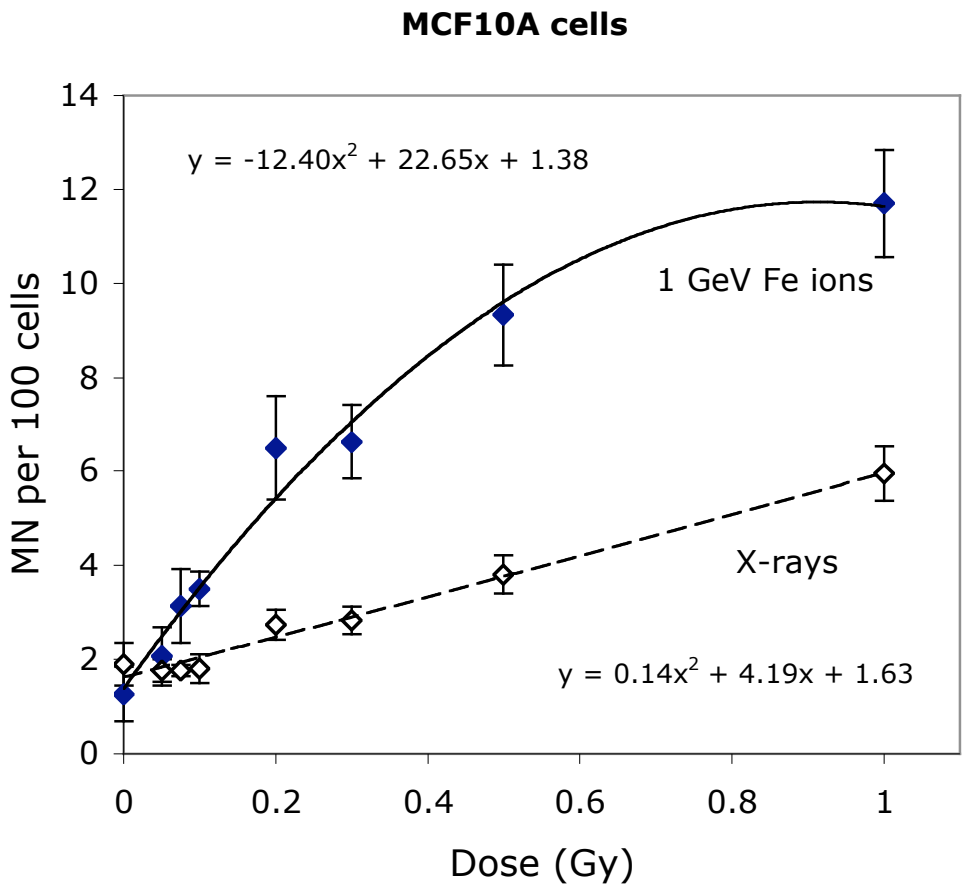
MCF10A cells
y = -12.40x2 + 22.65x + 1.38
1 GeV Fe ions
X-rays
y = 0.14x2 + 4.19x + 1.63
MN per 100 cells
Dose (Gy)
0
2
4
6
8
10
12
14
0
0.2
0.4
0.6
0.8
1

Figure 4.

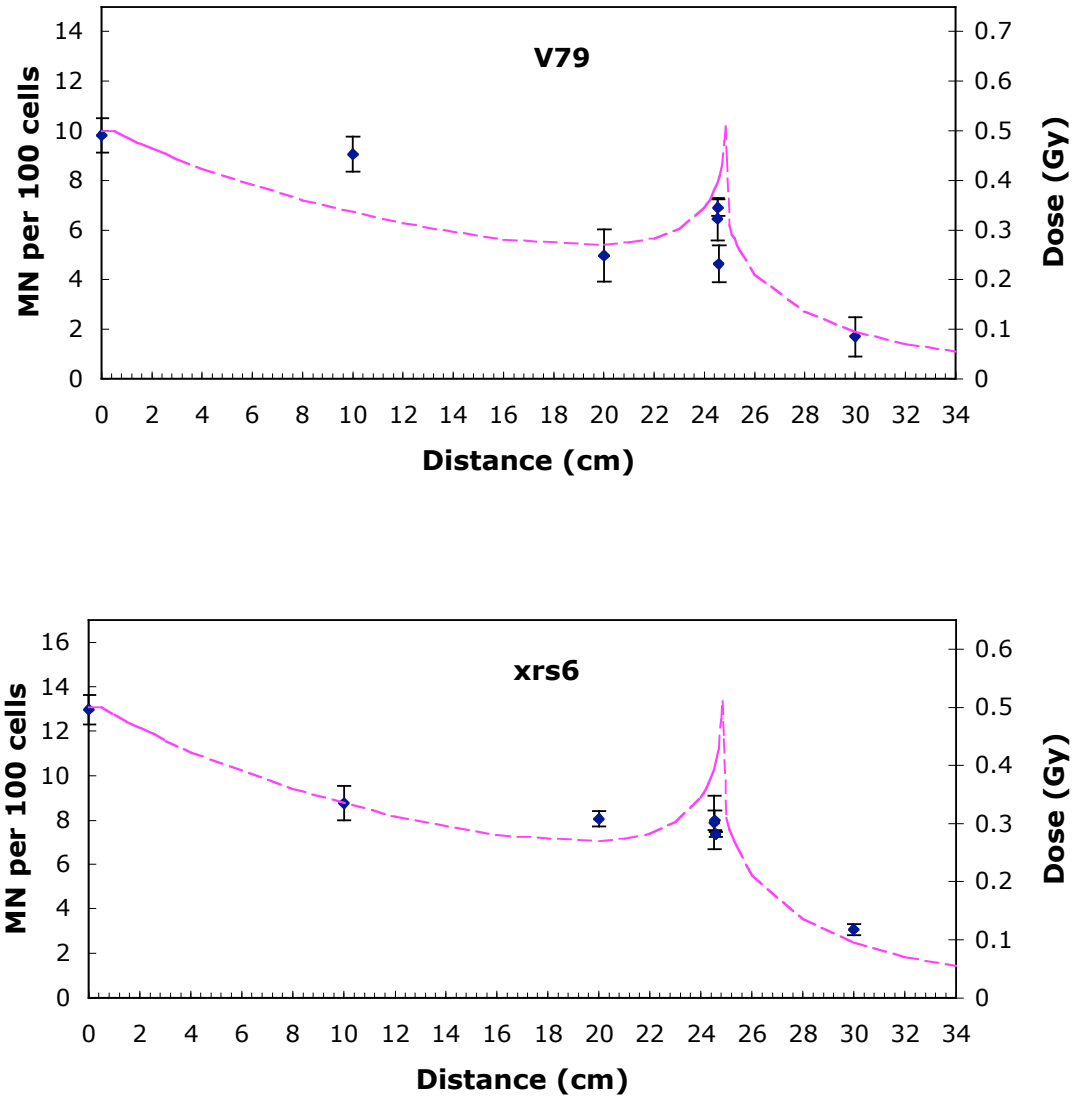
V79
MN per 100 cells
Dose (Gy)
Distance (cm)
xrs6
MN per 100 cells
Dose (Gy)
Distance (cm)

Figure 5.